DC 전력시스템에서의 Voltage Bus Conditioner의 제어기법 비교

論 文
55P-1-9

The Comparison of Two Control Algorithm for a Voltage Bus Conditioner in a DC Power Distribution System

羅 在 斗*·李 龍 根†
(Jae-Du La · Yong-Geun Lee)

Abstract - A Voltage Bus Conditioner (VBC) is used to mitigate the voltage transients on a common power distribution bus. The VBC described here utilises inductive storage and unlike its counter part with capacitive storage, it can employ the entire stored energy towards transients' mitigation. The performances of adaptive duty ratio control and sliding mode control have been compared. The simulation results (with the package SABER) indicate that the sliding mode control results in the shortest and the smallest bus voltage excursions.

Key Words : All-Electric Aircraft power system, Voltage bus conditioner, Adaptive control, Sliding mode control

1. Introduction

In the All-Electric Aircraft, electric power is utilised to drive aircraft subsystems instead of mechanical, hydraulic, and pneumatic power transfer systems [1]. The rapid technological advances in power electronics are much affecting the improvement of the performance of aircraft systems and their reliability. Also, the high voltage DC aircraft power system is becoming a performance benchmark in advanced aircraft applications. The selection of a high voltage DC power distribution offers the following advantages: 1) high efficiency, 2) high reliability, 3) power continuity, 4) fuel economy, and 5) improved personnel safety [1]-[2].

The All-Electric Aircraft power system is made up of generation systems, distribution systems, and loads connected together. After generating electrical energy from generation systems, distribution systems transfer electrical energy to the loads [1]. In addition, a large number of sizable loads take the form of power electronic converters. These power converters, when they are tightly regulated, appear as constant power loads and result in negative incremental input impedance. Under certain conditions the effect of such loads on the distribution system is to cause instability [2], [4]. Thus, power conditioner including an energy storage component and a bidirectional power converter is required to manage and control the power distribution system effectively, the converter effectively bringing the impedance of the generator/bus filter down to zero.

Power conditioners (also Voltage Bus Conditioner, VBC) have been widely investigated for compensation of reactive and harmonic currents in electrical power systems. These power conditioners could be divided into two types: voltage-storage and current-storage. One of the drawbacks of the voltage-storage power conditioner is that it inherently does not fully utilise the storage capacitor energy. The drawback of the current-storage power conditioner is large power losses of the storage inductor, however this can be overcome with the use of cryogenic power electronics and superconducting coils [3]-[4]. The current storage power conditioner is therefore seen as an attractive solution for All-Electric Aircraft power system.

The choice and implementation of the converter controller is very important for the achievement of a satisfactory performance level. The control techniques that have so far demonstrated an excellent performance in practical applications to the control of power converters are the adaptive control and sliding mode control [5]-[6]. In the proposed adaptive control, the controller automatically adjusts the compensator parameters whenever the system operating point, such as voltage, current and so on, changes. This control approach is based on small signal averaged model of the VBC. The controller consists of a second-order low-pass filter, an adaptive controller with a varying gain and a constant gain. In spite of the controller complexity, this control method has a wide control range with reasonable dynamics. In the general sliding mode

* 正 會 員 : The University of Birmingham, 博士課程
† 교신저자, 正會員 : 仁荷工業專門大學 電氣情報科學科 副敎授
E-mail : leeyong@inhatc.ac.kr
接受日字 : 2005년 10월 31일
最終完了 : 2006년 1월 10일

control, the control approach is associated with theoretical complexity and high frequency chattering. However, the sliding mode control provides large-signal stability, robustness, good dynamic response, and simple implementation. To reduce the chattering around the sliding surface, two sliding surface with the side bands is proposed. Both the proposed controllers were verified by means of Saber simulation.

2. Control Philosophy and Simulation Setup

The control philosophy employs the fact that, in order to maintain zero bus voltage variation, the voltage across the bus filter capacitor should be maintained constant. This translates in maintaining zero current through the filter capacitor C (Figure 1) and is achieved by compensating for the disturbance current.

The VBC should be a self-contained unit, as interference with other aircraft systems should be avoided. This implies that only non-invasive means for sensing should be employed. For the VBC, there are several possibilities. Firstly, the unit's input voltage could be sensed. The disadvantage is that, in order to estimate the disturbance current, the bus voltage needs to be differentiated, significantly compromising the noise immunity of the control loop. This ultimately results in the reduced bandwidth of the controller and therefore the resulting bus transients are inherently larger.

The second approach is to sense either the filter capacitor current or the current sourced by the VBC. Both approaches are functionally equivalent. The sensor does not need to be able to sense DC currents and an efficient current transformer can be used. In our simulations we focus on the second approach.

The operational requirements for the VBC refer to its functionality and it's interface to the voltage bus. Constant frequency operation is desirable, as it results in predictable switching harmonics injected into the bus. In our study we have employed an adaptive algorithm to vary the duty ratio with constant frequency, as such type of control. Another desirable feature of the VBC is to have high density and minimum switching losses. This could be achieved by reducing the average number of commutations (and/or soft commutation), yet instantaneously responding to system state changes, such as the flavour of sliding mode control explored here.

A synchronous machine is used as a generator in an aircraft system. A DC machine directly coupled to the engine shaft provides the excitation. The output voltage is controlled by modulating the excitation of the DC machine, which is a fairly slow process, usually with a bandwidth of less than 10Hz. The 400Hz three-phase output of the generator is rectified with full-wave rectifier followed by a differential mode second-order filter. The corner frequency of this filter is around 1kHz, providing ample attenuation of the low-frequency ripple. The important characteristics of this arrangement are two. Firstly, the rectifier does not allow reverse current flow into the generator. Secondly, the impedance and the corner frequency of the differential mode filter dominate the transients on the bus.

The constant power load in this study is a step-down (Buck) converter drawing 20A from the bus in steady state. The bandwidth of the controller is 1kHz. The buck converter is activated and deactivated by using squarewave for the reference. The rise time of this squarewave is adjusted so that the peak input current is twice the nominal current i.e. 40A, resulting in a peak power of 11kW.

The design of the VBC is based on the systems' anticipated needs for transients. In our particular application, a short pulsed-power load was rated at 10J, which is then also the energy storage capabilities of the storage inductor. The average current of the load was 20A, resulting in a value of the inductor L=50mH. The value of the filter capacitor is calculated from the allowable voltage ripple introduced onto the bus. Assuming a worst case value of 1% of the nominal voltage (no additional filtering is available), the filter capacitor is C=10F.

Lastly, the worst-case scenarios have been simulated here. This is the case when the bus is transiently loaded from 0% to 100%. Therefore, following a load turn-off, the steady-state voltage is at a level slightly above the nominal 270V. In practice this slowly converges to 270V to compensate for losses in the VBC unit.

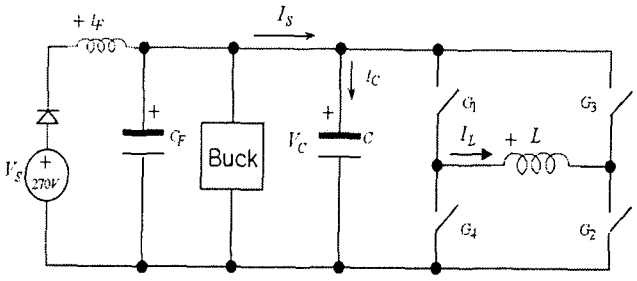

Fig. 1 Topology of the VBC with inductive storage.

3. Adaptive Control

Transfer function for the converter may be obtainedby writing down the averaged state equations, then linearising by considering small-signal perturbations [7]. Fig. 1 shows the simplified converter structure. Assuming that the ripple components of circuit waveform are small, the state space averaging equation for converter will be obtained as follows

$$\begin{bmatrix} \frac{\partial \bar{V}_C}{\partial t} \\ \frac{\partial \bar{I}_L}{\partial t} \end{bmatrix} = \begin{bmatrix} 0 & \frac{1-2D}{C} \\ -\frac{1-2D}{C} & 0 \end{bmatrix} \begin{bmatrix} \bar{V}_C \\ \bar{I}_L \end{bmatrix} + \begin{bmatrix} \frac{1}{C} \\ 0 \end{bmatrix} \bar{I}_S \quad (1)$$

where D is the duty ration of switch G_1, G_2 and $\overline{V_C}$ is the average DC bus voltage. Also, $\overline{I_L}$ is the average storage inductor current and $\overline{I_S}$ is the average source current.

From equation (1) and with the definition of the relevant control variables, the small-signal averaged model of the converter with duty ratio control is:

$$\begin{bmatrix} \tilde{V}_C \\ \tilde{I}_L \end{bmatrix} = \frac{\begin{bmatrix} -\frac{2s\bar{I}_L}{C} - \frac{2\bar{V}_C(1-2\bar{D})}{LC} \\ \frac{2s\bar{V}_C}{L} - \frac{2\bar{I}_L(1-2\bar{D})}{LC} \end{bmatrix} \tilde{D} + \begin{bmatrix} \frac{s}{C} \\ 0 \end{bmatrix} \tilde{I}_S}{s^2 + \frac{(1-2\bar{D})^2}{LC}} \quad (2)$$

where quantities with tilde denote small-signal variable (AC component) and quantities with a bar denote averaged variables (DC component). The average value of the duty ratio is 0.5 such that, for lossless VBC, no average current is injected into the buss in steady-state.

The transfer function for the bus voltage is:

$$\tilde{V}_C = \frac{\frac{\tilde{I}_S}{C}s - 2\left\{\frac{\bar{I}_L}{C}s - \frac{(2\bar{D}-1)\bar{V}_C}{LC}\right\}\tilde{D}}{s^2 + \frac{(2\bar{D}-1)^2}{LC}} \quad (3)$$

By expressing the voltage across the filter capacitor $\tilde{V}_C$ and equating to zero, the control law can be shown to be:

$$\tilde{D} = \tilde{I}_S \frac{1}{2\bar{I}_L\left\{1 - \frac{(2\bar{D}-1)\bar{V}_C}{L\bar{I}_L}\frac{1}{s}\right\}} \quad (4)$$

Equation (4) indicates that the controller will not only respond instantaneously to disturbance current $\tilde{I}_S$, but also will adjust the controller gain in response to operating point deviations such as storage current $\overline{I_L}$ and average bus voltage $\overline{V_C}$.

The disturbance signal $\tilde{I}_S$ is obtained from the original current through a second order critically damped filter with corner frequency at 10kHz. This determines the bandwidth of the controller and is far above the typical dynamics of the electrical system. The stability of the system is based on the presumption that the VBC does not overcompensate for bus disturbances. This translates into the filter gain no larger than unity. Significantly smaller gains will compromise the performance of the VBC. In our simulations we have conservatively reduced this by 5% to allow for production tolerances of the sensor gain.

A second auxiliary loop is needed to maintain steady-state current stored in the inductor. The transfer function of the converter for the storage current is:

$$\frac{\tilde{I}_L}{\tilde{D}} = \frac{\frac{2\bar{V}_C}{L}s - \frac{2\bar{I}_L(1-2\bar{D})}{LC}}{s^2 + \frac{(1-2\bar{D})^2}{LC}} \quad (5)$$

Converters with transfer functions of the form (5) are notoriously difficult to control, due to the pair of un-damped complex poles, the frequency of which varies with the operating point. In addition, the phase relationship reverses, depending on whether the inductor sources or sinks energy from the bus. In this application, however, the corresponding gain for the compensator should be considerably smaller than that in eq. (3), since the two loops have conflicting objectives. Simple proportional control is then sufficient to maintain the prescribed inductor current and thus the desired level of energy storage.

We chose the closed-loop gain of the auxiliary loop to be ten times smaller than that of the main loop as a compromise between sufficiently low steady-state error for the storage inductor current and minimum interference of the storage control loop. Assuming conditions not very far from the steady-state ($\overline{V_C}$=270V, L=50mH, C=10F, $\overline{I_L}$ =20A) the ratio between the (open loop) gains is 0.0027. The gain for the storage current should then be 0.00027 within the control bandwidth. A low-pass filter was used as a compensator. Its DC gain is 0.0027 (making the gains of the two loops equal and low frequencies) and a corner frequency (1kHz) which is a decade below the intended controller bandwidth. With this arrangement the auxiliary loop does not interfere with the operation of the main loop, but will still provide very small error for the storage current.

The implementation of the adaptive control is shown in the block diagram in Fig. 2.

In order to verify the performance of the proposed control, some simulations were made by SABER packageand the associated simulation conditions are described above section II. The simulation results are shown in Fig. 3. The voltage excursions on the bus voltage (nominal of 270V, bottom trace) are between 300V and 210V (at constant power load turn-on). The turn-on transitions are the most severe, but are fully damped within 2ms. These excursions could be further limited by increasing the bandwidth of the filter for the disturbance current (here 10kHz) which, according to eq. (3), determines the bandwidth of the controller. This however could pass too much switching ripple, causing the model

to collapse and leading to commutation failure. It should be noted that the turn-on excursions are inherently larger as the bus is subjected to a disturbance current which is twice that of the current capabilities of the VBC.

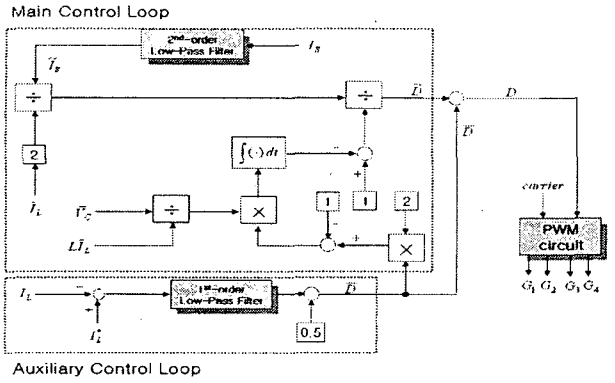

Fig. 2 Implementation of adaptive control

The average storage current is just below 20A (middle trace) and strives slowly to its nominal value after each commutation. It increases more steeply after load turn-off to absorb the current from the filter inductor LF.

The duty ratio (top trace) deviates around a steady-state value just below 0.5 to compensate for losses in the switches and the inductor. Also, the largest excursions occur at load turn-on, as the available storage current cannot fully compensate for the larger disturbance current. For the duration of this instant, the VBC sources the maximum available current to the bus. This is demonstrated by duty ratio.

of operation:

$$u_1 = \begin{cases} +1 & \text{for } G_1 \text{ and } G_2 : \text{ON} \quad \text{inductor charge} \\ 0 & \text{for } G_2 \text{ and } G_4 : \text{ON} \quad \text{freewheeling } I_L \end{cases}$$

$$u_2 = \begin{cases} -1 & \text{for } G_3 \text{ and } G_4 : \text{ON} \quad \text{inductor discharge} \\ 0 & \text{for } G_2 \text{ and } G_4 : \text{ON} \quad \text{freewheeling } I_L \end{cases} \quad (6)$$

the freewheeling state being interchangeable.

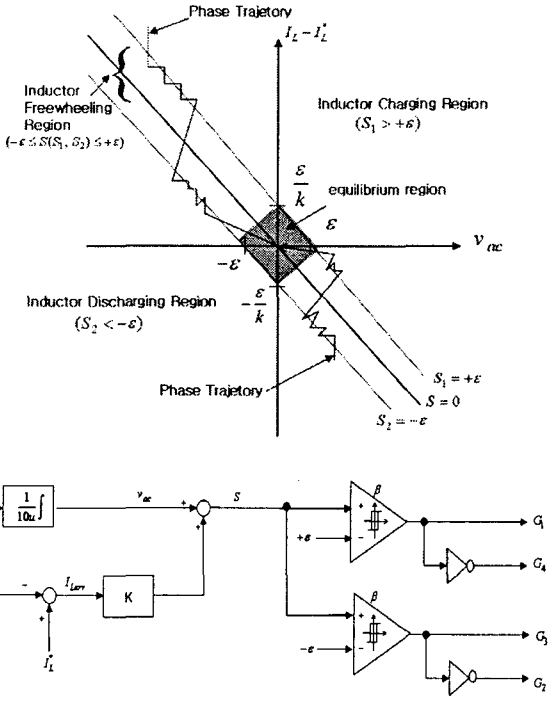

Fig. 4 Implementation of sliding mode

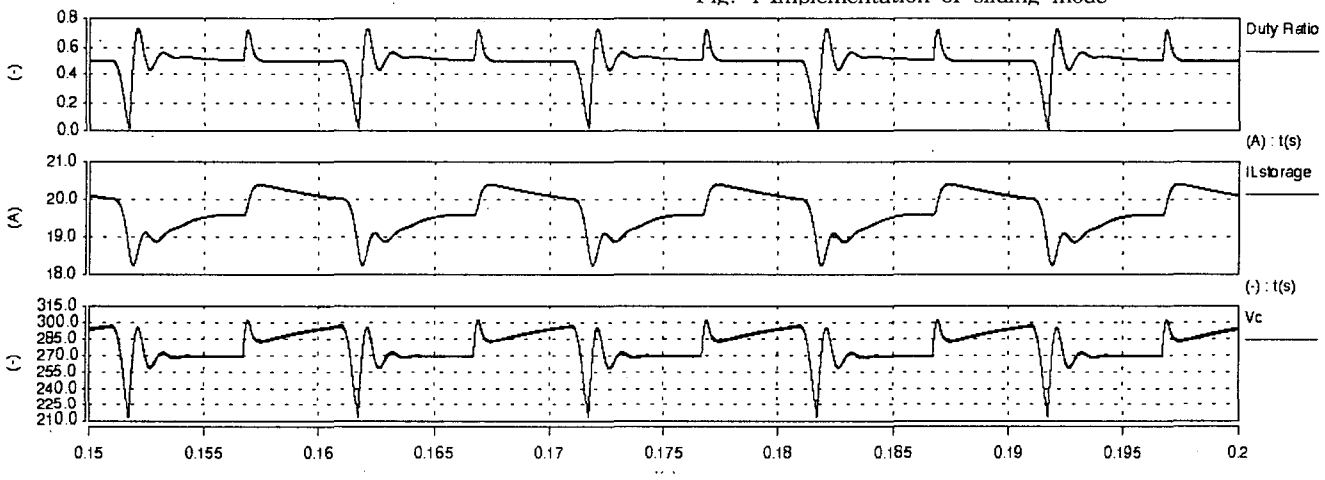

Fig. 3 Simulation result for adaptive control.

4. Sliding Mode Control

The SM control was designed to reduce the number of commutations and to provide the fastest response possible. There are three meaningful switch combinations (Fig. 1) for the converter, which can be described with two modes

By the sliding mode approach proposed by Ramirez [8], the following state-space equation can be obtained from Fig. 1.

$$\begin{bmatrix} \frac{\partial V_C}{\partial t} \\ \frac{\partial I_L}{\partial t} \end{bmatrix} = \begin{bmatrix} 0 & -\frac{1}{C} \\ \frac{1}{L} & 0 \end{bmatrix} \begin{bmatrix} V_C \\ I_L \end{bmatrix} u_\gamma + \begin{bmatrix} \frac{I_S}{C} \\ 0 \end{bmatrix} \quad (7)$$

where $\text{Mode 1}: \gamma = 1,$ $\text{Mode 2}: \gamma = 2$

The control sliding surface is of the form:

$$S = v_{ac} + k(I_L^* - I_L) = 0 \quad k - \text{gain for control of } I_L \quad (8)$$

with side bands:

$$S_1 = v_{ac} + k(I_L^* - I_L) = +\varepsilon \quad \text{and}$$

$$S_2 = v_{ac} + k(I_L^* - I_L) = -\varepsilon \quad (9)$$

where I_L^* is the desired storage current, I_L is its current value and v_{ac} is the instantaneous value of the AC component of the bus voltage.

The existence condition of sliding mode requires that all state trajectories near the surface be directed toward the sliding plane. Mathematically this is expressed with:

$$\frac{\partial S_1}{\partial t} > 0 \ \text{if} \ 0 < S_1 < \varepsilon \ \text{and} \ \frac{\partial S_1}{\partial t} \le 0 \ \text{if} \ S_1 > \varepsilon \quad (10)$$

for Mode 1 and

$$\frac{\partial S_2}{\partial t} < 0 \ \text{if} \ -\varepsilon < S_2 < 0 \ \text{and} \ \frac{\partial S_2}{\partial t} > 0 \ \text{if} \ S_2 < -\varepsilon \quad (11)$$

for Mode 2.

Using equation (9) and keeping in mind that in Mode 2 the current IS is negative, equation (10), (11) poses that:

$$k > \frac{L}{C}\frac{I_S - I_L}{V_C} \ \text{if} \ S_1 > \varepsilon \ \text{and} \ \frac{I_S}{C} > 0 \ \text{if} \ 0 < S_1 < \varepsilon \quad (12)$$

for Mode 1 and

$$k > \frac{L}{C}\frac{I_S - I_L}{V_C} \ \text{if} \ S_2 < -\varepsilon \ \text{and} \ \frac{I_S}{C} < 0 \ \text{if} \ -\varepsilon < S_2 < 0 \quad (13)$$

for Mode 2.

All the conditions above are satisfied as long as the disturbance current is smaller in amplitude than the storage current. The inability of the controller to reach S=0 with such operating points are natural and are associated with the limited storage capabilities of the inductor. However, the controller will still provide the maximum available excitation in order to impede bus voltage variations.

With the above arrangement the switch states will oscillate around surface S1 (which is offset from S by) within the band, charging the storage inductor when the ac component of the bus voltage v_{ac} is bigger than zero (voltage raising). A complementary statement is true for falling bus voltage and sliding surface S2. This is illustrated in Fig. 4, left. Commutation will cease when the bus voltage is close to the surface S and changing slowly. A block diagram of a controller with such functionality is also shown in Fig. 4.

The bus voltage variation is limited by narrowing the sliding surfaces offset. In our design of the controller, we have assumed a very conservative value for variation on the voltage bus of 1V. This results in $\epsilon = \pm 1$, in accordance with equation (9).

The control gain of the loop for the storage is determined again from equation (9) by substituting $|\epsilon| = 1$. Assuming that there is no variation on the voltage bus and that the controller will be active when the storage current deviates by more than 2 A (10%) from its desired value, the gain k is obtained:

$$S = 0 + k \times |2| = |1| \ \therefore \ k = 0.5 \quad (14)$$

The frequency of oscillation ('chattering') around S1 or S2 is determined by the width of the hysteresis band. In Mode 1, close to surface S1, the chatter frequency is:

$$|f_s| = \left| -\frac{I_S(L(I_S - I_L) - kCv_{ac})}{C\beta(LI_L + kCv_{ac})} \right| \quad (15)$$

In Mode 2, the chatter frequency is:

$$|f_s| = \left| \frac{I_S(L(I_S + I_L) + kCv_{ac})}{C\beta(LI_L + kCv_{ac})} \right| \quad (16)$$

Solving equation (16) for maximum frequency of 100 kHz results in hysteresis bandwidth $\beta = 1.049$ for Mode 1 and $\beta = 1.050$ for Mode 2.

The bus voltage can be expressed with its DC and AC components as:

$$V_C = V_{DC} + v_{ac} = V_{DC} + \frac{1}{C}\int I_C dt \quad \therefore v_{ac} = \frac{1}{C}\int I_C dt \quad (17)$$

Equation (11) is used to separate the DC and the AC components, so that the controller responds only to AC variations on the bus, as can be seen from Fig. 4, right.

The simulation results by SABER package, together with the simulation condition of section II, are shown in Fig. 3. The simulation results are shown in Fig. 5. The bus voltage excursions (bottom trace) are considerably smaller and better damped. The average value of the storage inductor current (middle trace) is maintained at 20A, however the variations are larger. The waveform is obviously less repeatable than for the other types of control, which is attributed to the discrete nature of the controller operation. However, this could be improved by increasing the gain k, that would lead to increased number

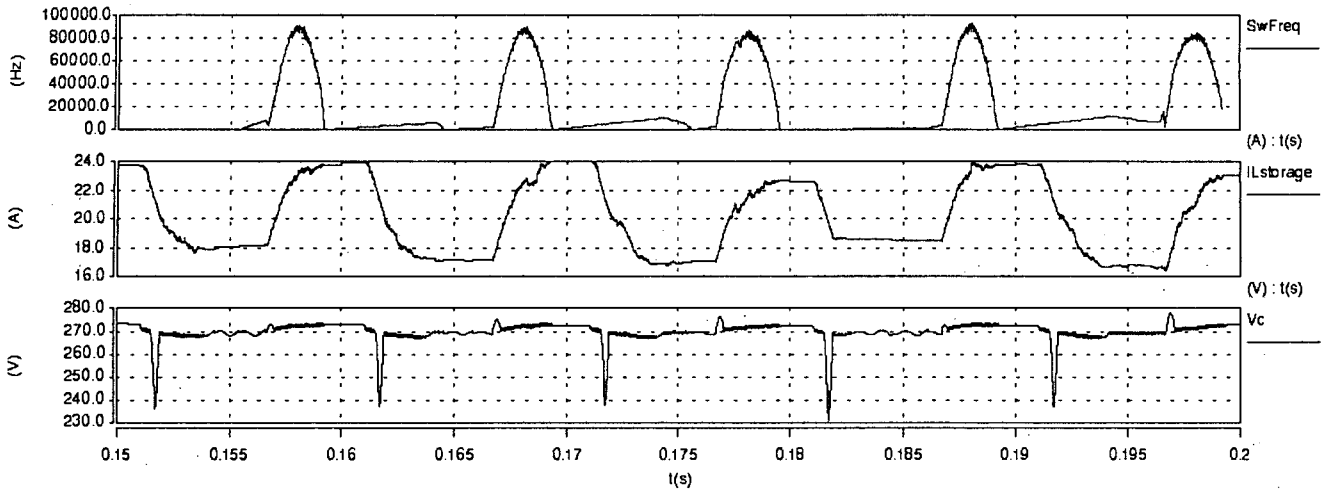

Fig. 5 Simulation result for sliding mode control.

of commutations.

The commutation frequency (top trace) rises to just below 90kHz when the load is turned off, in order to absorb the energy stored in the filter inductor. During load turn on, the controller generates a very short burst of commutation instances, limiting the bus voltage transition.

3. Conclusion

The type of voltage bus conditioner (with inductive storage) described here utilises all of the stored energy, unlike its counterpart with capacitive storage. Three types of control have been designed and simulated.

The adaptive duty-ratio control was used as a performance benchmark. It has the advantage of predictable current harmonic content being injected into the voltage bus. The controller requires digital implementation with which most modern DSPs can cope. The resulting voltage excursions are well within the prescribed standards, and are fully damped within less than 2ms, despite the severe test conditions of transitional loading of the bus with excessive current [9].

The simulated sliding mode controller resulted in even better performance. The type of controller benefits from robust convergence and is devoid of chattering in steady-state, a problem common for most sliding-mode controllers. As a result, the switching frequency of the devices is well below one fifth of that for the duty-ratio control. The bus voltage excursions approach the theoretically minimum values and are very well damped.

Although the system described here has in its scope an aerospace application, the general principles and conclusions that can be drawn for the performance of the controllers are clearly applicable to other systems, where critical equipment needs to be protected from bus voltage variations in a dynamic and noisy environment.

References

[1] D. Segrest, W. W. Cloud, "Evolution and Development of High Voltage (270 Volt) DC Aircraft Electric Systems in the United States", SAE Transaction on Journal of Aerospace, VOL. 90, pp 51-63, 1981

[2] Ali Emadi, Babak Fahimi, and Mehrdad Ehsani, "On the Concept of Negative Impedance Instability in the More Electric Aircraft Power system with Constant Power Loads", Society of Automotive Engineers (SAE) Journal, Paper No. 1999-01-2545, 1999

[3] Mika Salo and Heikki Tuusa, "A Novel Open-Loop Control Method for a Current-Source Active Power Filter", IEEE Transactions on Industrial Electronics, VOL. 50, No. 2,313321, April 2003.

[4] Andrew J Forsyth and Awang Jusoh, "Simulation of an Active Damping Device for DC Power Networks", Society of Automotive Engineers Conf., Paper No. 2002-01-3191, 2002

[5] Claudia Hernandez, Nimrod Vazquoz, and Victor Cardenas, "Sliding Mode Control for a Single Phase Active Filter", Power Electronics Congress, CIEP 98. VI IEEE International, pp.171 - 176, 12-15 Oct. 1998

[6] Shoji Fukuda, and Hirofumi Kamiya, "Adaptive Learning Algorithm Assisted Current Control for Active Filters", Industry Applications Conference, 2001. Thirty-Sixth IAS Annual Meeting. Conference Record of the 2001 IEEE, VOL 1,179 185, Sept. 2001

[7] Middlebrook and Cuk, "A General Unified Approach to Modelling Switching Converter Power Stages", International Journal of Electronics, VOL 24-6, 1977

[8] H. Sira-Ramirez, "Nonlinear Pulse Width Modulation Controller Design", Variable Structure Control for Robotics and Aerospace Application/K.K.D. Young, 1993, Elsevier Science.

[9] MIL-STD-704E, Military Standard, Aircraft Electric Power Characteristics, May 1, 1991

저 자 소 개

나 재 두 (羅 在 斗)

1970년 10월 10일생. 1994년 인천대학교 전기공학과 졸업. 1996년 인하대학교 전기공학 졸업(석사). 2003.8. G&W Technologies, 선임연구원. 2003.9 - 현재, 영국 The University of Birmingham, EECE, 박사과정.

Tel : +44-121-414-3150, E-mail : jxl399@bham.ac.uk

이 용 근 (李 龍 根)

1960년 11월 6일생. 1985년 인하대학교 전기공학과 졸업. 1989년 미국 University of Missouri-Columbia 전기공학 졸업(석사). 1993년 동 대학원 졸업(공박). 1995. 3 - 현재 인하공업전문대학 전기정보과학과 부교수.

Tel : 032)870-2196, E-mail : leeyong@inhatc.ac.kr